Multimerization of Restriction Fragments by Magnesium-Mediated Stable Base Pairing between Overhangs: A Cause of Electrophoretic Mobility Shift†

Hideki Tagashira,‡ Mitsunori Morita,‡ and Takashi Ohyama*,‡,§

Department of Biology, Faculty of Science and Engineering, and High Technology Research Center, Konan University, 8-9-1 Okamoto, Higashinada-ku, Kobe 658-8501, Japan

Received June 17, 2002; Revised Manuscript Received July 30, 2002

ABSTRACT: The electrophoretic mobility shift assay (EMSA) or simply the "gel shift assay" is one of the most sensitive methods for studying the ability of a protein to bind to DNA. EMSAs are also widely used to investigate protein- or sequence-dependent DNA bending. Here we report that electrophoresis using physiological concentrations of Mg^{2+} can cause a mobility shift of restriction fragments in nondenaturing polyacrylamide gels as the overhangs form stable base pairs. This phenomenon was observed at even 37 °C. The retardation was, however, more pronounced at low temperatures, where a three-nucleotide overhang 5′-GAC also caused a mobility shift. The stability of the pairing was generally high when the overhangs of four nucleotides display high GC content, while the mobility shift caused by 5′-AATT was greater than those caused by 5′-GATC, 5′-TCGA, and 5′-CTAG. This observation should be taken into account to avoid misinterpretation of the data when the EMSA, especially the circular permutation gel mobility shift assay, is performed using a running buffer that contains Mg^{2+} ions. The stable adhesion between short overhangs may present an important basis for genome stability and many genetic processes occurring in living cells.

Electrophoresis of DNA through polyacrylamide gels is a standard method in molecular biology. It is used not only to separate, identify, and purify DNA fragments (*1*) but also to detect protein−DNA interactions (*2*), as well as the presence of unusual DNA structures such as intrinsically curved and cruciform DNA structures (*3, 4*). The EMSA[1] is based on the phenomenon that the DNA fragments bound by protein(s) or having an unusual DNA structure migrate more slowly in nondenaturing polyacrylamide gels than "naked" or ordinary DNA fragments of the same size (*2*, *3*). Furthermore, if the protein induces a DNA bend on binding, the protein−DNA complex migrates more slowly in the gel than the nonbent complex of the same mass (*5*).

The center of the intrinsically curved DNA, or the site of the protein-induced DNA bend, is easily determined using circularly permuted DNA fragments. This technique, which was developed by Wu and Crothers and is called circular permutation analysis (*5*), makes use of the phenomenon that bent DNA slows the movement, with the effect being more pronounced when the bend is positioned in the center of a DNA molecule as opposed to the ends. Using this analysis, a great many intrinsically curved DNA structures and protein-induced DNA bends have been found (*6*, *7*). This technique, however, has not taken into account end-to-end DNA interaction as a possible cause of the band shift. If this is the case, it has the potential to result in misinterpretation of the data obtained from this very widely used technique.

We have found that several restriction fragments with cohesive ends displayed anomalous electrophoretic behavior in nondenaturing polyacrylamide gels when Mg^{2+} was present. The changes in DNA migration have been explained as being due to intermolecular or intramolecular end-to-end interaction. It is known that the Mg^{2+} alleviates electrostatic repulsive interactions between phosphates, thereby stabilizing base pairing and base stacking (*8*). Although Mg^{2+} is also known to influence DNA conformation (*9*−*14*), its effect on the terminal ends of DNA restriction fragments has not been fully understood. Since the EMSA has sometimes been carried out in the presence of Mg^{2+}, this phenomenon may have resulted in misinterpretation of the data. On the other hand, the finding of the Mg^{2+}-mediated stable base pairing between short overhangs may help solve some of the unsettled problems in genetic research.

MATERIALS AND METHODS

Construction of Plasmids. Plasmids pPRT-5/4 and pPRT-5/3 were made as follows. At first, each of the following sets of oligonucleotides was annealed in a solution containing 100 mM NaCl: 5′-GGGAATTCGGCCGCTTAAGTCCGG-ATCCTCGAGGCGCCAAGCTTCTAGACGCGTCCC-3′ (a), 5′-GGGACGCGTCTAGAAGCTTG-3′ (a′), 5′-ATCG-ACAGTGTCATCGATTAATGGGGCCCGCTTAGCGG-ACCGCCTGAGGACACGTGAT-3′ (b), and 5′-ATCACGT-GTCCTCAGGCGGTC-3′ (b′). The molecules were subse-

† This work was supported in part by a Grant-in-Aid for Scientific Research from the Ministry of Education, Culture, Sports, Science and Technology of Japan, NIG Cooperative Research Program, and the Hirao Taro Foundation for Academic Research (to T.O.).

* To whom correspondence should be addressed. E-mail: ohyama@base2.ipc.konan-u.ac.jp. Telephone or fax: +81 78 435 2547.

‡ Faculty of Science and Engineering.

§ High Technology Research Center.

[1] Abbreviations: AFM, atomic force microscopy; BAP, bacterial alkaline phosphatase; EMSA, electrophoretic mobility shift assay; dNTPs, deoxyribonucleoside triphosphates; TB, Tris-borate; TBE, Tris-borate-EDTA; TAE, Tris-acetate-EDTA.

10.1021/bi026308f CCC: $22.00
Published on Web 09/14/2002

quently precipitated with ethanol and dried. The recessed 3′-termini of the a−a′ and b−b′ duplexes were filled with dNTPs using T4 DNA polymerase. The resulting blunt-ended duplexes were extracted with phenol, precipitated with ethanol, washed with 70% ethanol, and dried. Each duplex was then cloned between the *Eco*RI and *Hin*dIII sites of pUC19 that had been made blunt-ended. We screened the recombinant plasmids carrying each duplex as a tandem dimer and designated them pPRT-5/4 and pPRT-5/3, respectively. To construct pRES, we used the following oligonucleotides: 5′-AATTCGGGCCCCACTGCGTCGATATC-GGGCCCCACTGCGTCTGCA-3′ (c) and 5′-GACGCAGT-GGGGCCCGATATCGACGCAGTGGGGCCCG-3′ (c′). The c−c′ duplex was prepared in the same manner described above and cloned into pUC19 cut with *Eco*RI and *Pst*I.

Subsequently, the fragment generated by digestion of pBR322 with the restriction enzymes *Pst*I and *Pvu*I (nucleotides 3612−3734) was made blunt-ended by end filling with dNTPs using T4 DNA polymerase. This fragment was then inserted into the *Sma*I site of pPRT-5/4 or the *Eco*RV site of pPRT-5/3 and pRES to generate pPRT-5/4B, pPRT-5/3B, and pRES-B. By digesting the plasmids with various restriction enzymes, we produced 21 DNA fragments. The construct pPRT-5/4U was created by inserting the *Bbi*II and *Ssp*I fragment of pUC19 (nucleotides 2237−2503) into *Sma*I-cleaved pPRT-5/4 by blunt-end ligation. The DNA fragments with one blunt end and the other 5′-CGCG overhang were prepared from pPRT-5/4B and pPRT-5/4U using *Ssp*I and *Mlu*I, *Eco*O109I (and T4 DNA polymerase) and *Mlu*I, or *Dra*I and *Mlu*I.

Enzyme Reactions. Digestion of DNA with restriction enzymes, fill-in reaction with T4 DNA polymerase, removal of the 3′-overhang with S1 nuclease (or T4 DNA polymerase), removal of the 5′-terminal phosphate with bacterial alkaline phosphatase (BAP), and 5′-end labeling with [γ-^{32}P]-ATP using T4 polynucleotide kinase were performed using conventional methods (*1*). Unless otherwise indicated, enzyme-treated DNA fragments were extracted from each reaction mixture with phenol, precipitated with ethanol, washed with 70% ethanol, and dried. In the end labeling reaction, the DNA-containing aqueous solution obtained by phenol extraction was loaded onto a Micro Spin G-25 column (Amersham Pharmacia Biotech) to separate the labeled DNA fragments from residual [γ-^{32}P]ATP, and the eluate was treated as described above. DNA ligation with T4 DNA ligase was carried out as follows. First, we prepared 8 μL of a solution containing 960 ng of the DNA fragments, 66 mM Tris-HCl (pH 7.5), 10 mM $MgCl_2$, 1 mM DTT, and 0.1 mM ATP. The reaction mix was then incubated at 5 °C for 20 min. Then, 2 μL of the T4 DNA ligase solution comprised of 7 units of the enzyme and the same buffer described above was added. The reaction mixture was then incubated at 5 °C for 90 min. The reaction was stopped as described above, and the products were resuspended in 10 mM Tris-HCl (pH 7.5). Approximately 250 ng of each ligation product was electrophoresed.

Measurement of Electrophoretic Mobility. For polyacrylamide gel electrophoresis in the presence of Mg^{2+}, approximately 300 ng of the purified DNA fragments (as well as marker DNA fragments) was dissolved in $^1/_2\times$ TB [45 mM Tris-borate (pH 8.3)] containing 1 or 10 mM $MgCl_2$. The samples were then electrophoresed on 7.5% polyacrylamide (29:1 acrylamide:bisacrylamide ratio) gels at 5, 20, or 37 °C. The gels contained, and the running buffers were comprised of, $^1/_2\times$ TB with 1 or 10 mM $MgCl_2$. The control experiment was carried out at 5 °C in the absence of Mg^{2+}. The gel contained, and the buffer was comprised of $^1/_2\times$ TB. The electrophoretic field across the gels was maintained at 5.7 V/cm. After electrophoresis, gels were stained with ethidium bromide. The buffer solution was pumped between the electrode compartments at a rate of ∼1200 mL/h. In addition, the contents of each compartment were stirred during electrophoresis (*14*). The agarose gel electrophoresis performed to detect DNA ligation products was carried out in $^1/_2\times$ TBE [45 mM Tris-borate and 1 mM EDTA (pH 8.3)] using a 1.5% agarose gel.

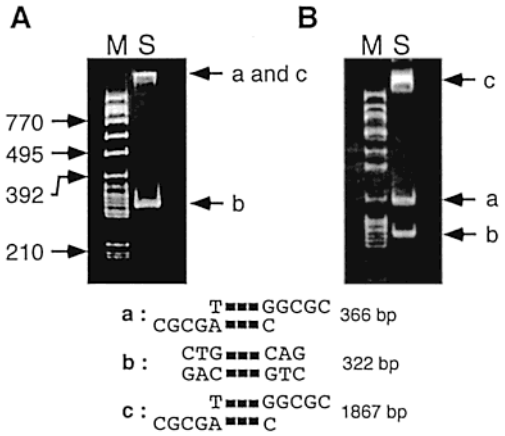

FIGURE 1: Electrophoretic anomaly observed for a DNA fragment with cohesive ends in the presence of Mg^{2+}. A digest of pUC19 with *Hae*II and *Pvu*II was subjected to nondenaturing polyacrylamide gel electrophoresis using 7.5% gels in the presence (A) or absence (B) of 10 mM $MgCl_2$. The sample and marker (mixture of *Hin*cII digest of phage ϕX174 DNA and *Hae*III digest of the DNA) were loaded onto lanes S and M, respectively. The DNA fragments are shown schematically.

Preparation of the Diluted Samples. Three microliters of the starting sample contained 0.3 ng of 5′-end-labeled fragment 10 in $^1/_2\times$ TB and 1 mM $MgCl_2$. Without a change in the concentration of each component, 3 μL of each of the second, third, and fourth samples were prepared to additionally contain 3, 30, and 300 ng of unlabeled fragment 10, respectively.

RESULTS

Initial Finding. It was observed initially that the 366 bp *Hae*II fragment of pUC19 migrated unexpectedly slowly in a nondenaturing polyacrylamide gel when the running buffer contained 10 mM Mg^{2+} (Figure 1A). The fragment migrated to the same position as that of the 1867 bp fragment. This fragment, however, migrated almost normally in a conventional nondenaturing polyacrylamide gel that did not contain Mg^{2+} (Figure 1B; the observed slight migration shift was presumably caused by a bent DNA structure in the fragment). Thus, it was evident that the presence of Mg^{2+} caused the band shift. Since a 322 bp DNA fragment with blunt ends did not show anomalous migration, we speculated that the Mg^{2+}-mediated interaction between the overhangs was implicated in the phenomenon. To substantiate this hypothesis, we performed a systematic study.

The Electrophoretic Anomaly Was Pronounced with High $MgCl_2$ Concentrations and at Low Temperatures. For this

Table 1: Restriction Fragments Used in This Study

NO.	Fragment Structure[a]	Size (bp)[b]	Restriction enzyme employed
1	AATTCGGGCC---CCGGG GCCGG---GGCCCTTAA	176	*Eco* R I
2	GGCCGCTTA---AATTC CGAAT---TTAAGCCGG	176	*Eco* 52 I
3	TTAAGTCCG---GCCGC CAGGC---CGGCGAATT	176	*Afl* II
4	CCGGATCCT---TAAGT TAGGA---ATTCAGGCC	176	*Mro* I
5	GATCCTCGA---GTCCG GAGCT---CAGGCCTAG	176	*Bam* H I
6	TCGAGGCGC---GATCC CCGCG---CTAGGAGCT	176	*Xho* I
7	GCGCCAAGC---TCGAG GTTCG---AGCTCCGCG	176	*Ban* I
8	AGCTTCTAG---CGCCA AGATC---GCGGTTCGA	176	*Hin*d III
9	CTAGACGCG---AGCTT TGCGC---TCGAAGATC	176	*Xba* I
10	CGCGTCCCG---CTAGA AGGGC---GATCTGCGC	176	*Mlu* I
11	GTGTCA---CGACA ACAGT---GCTGTC	180	*Pfl* F I
12	CGATTAA---GTCAT TAATT---CAGTAGC	179	*Cla* I
13	TAATGGG---TCGAT TACCC---AGCTAAT	179	*Psh* B I
14	GGCCCGCT---AATGG GGCGA---TTACCCCG	178	*Eco* O109 I
15	TTAGCGGA---CCCGC CGCCT---GGGCGAAT	178	*Bpu* 1102 I
16	GACCGCCT---TAGCG GCGGA---ATCGCCTG	178	*Cpo* I
17	TGAGGACA---CCGCC CCTGT---GGCGGACT	178	*Eco* 81 I
18	CACGTGATA---GAGGA ACTAT---CTCCTGTGC	177	*Afl* III
19	GGGCCCCACT---ATATC GGTGA---TATAGCCCGG	139	*Hga* I
20	CCACT---TATCGGGCC CCGGGGTGA---ATAGC	140	*Apa* I
21	TCGAT---CGGGCCCCACTGCG GGGTGACGCAGCTA---GCCCG	135	*Tsp* R I

[a] Structures of only the terminal regions are shown. The remainder of each DNA is depicted using a dotted line. [b] Only the double-stranded portion is counted.

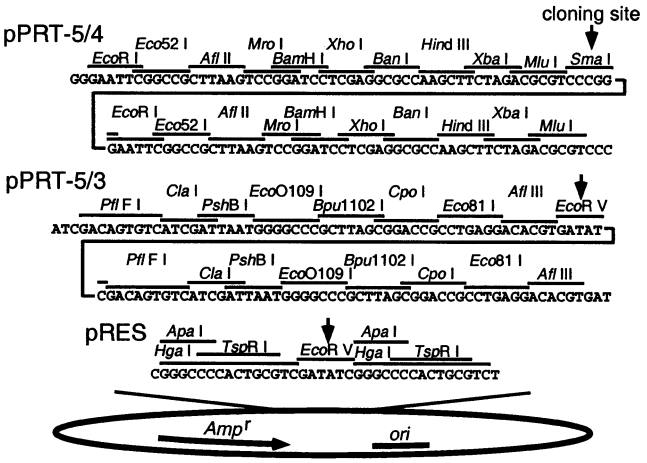

FIGURE 2: Plasmid vectors used in this study.

study, we constructed plasmids pPRT-5/4, pPRT-5/3, and pRES (Figure 2) and cloned the 123 bp *Pst*I−*Pvu*I fragment of pBR322 into the *Sma*I site of pPRT-5/4, or the *Eco*RV site of pPRT-5/3 and pRES. The resulting plasmids were digested with the restriction enzymes indicated in the schema of each plasmid structure. This generated 21 DNA fragments with different cohesive ends (Table 1). The electrophoretic behavior of the resulting fragments in the presence of Mg^{2+} is shown in Figure 3. Several fragments displayed the electrophoretic anomaly, and this was more pronounced at high $MgCl_2$ concentrations and at low temperatures. In the electrophoresis at 5 °C with 10 mM $MgCl_2$, the *Eco*52I (5′-GGCC overhang, lane 2), *Mro*I (5′-CCGG overhang, lane 4), *Ban*I (5′-GCGC overhang, lane 7), *Hin*dIII (5′-AGCT overhang, lane 8), *Mlu*I (5′-CGCG overhang, lane 10), *Afl*III (5′-CGTG and 5′-CACG overhangs, lane 18), *Hga*I (5′-GGGCC and 5′-GGCCC overhangs, lane 19), *Apa*I (3′-CCGG overhang, lane 20), and *Tsp*RI (3′-GGGTGACGC and 3′-GCGTCACCC overhangs, lane 21) fragments barely entered the gel. The *Eco*O109I (5′-GGC and 5′-GCC overhangs, lane 14), *Eco*RI (5′-AATT overhang, lane 1), *Bam*HI (5′-GATC overhang, lane 5), *Cpo*I (5′-GAC and 5′-GTC overhangs, lane 16), *Xho*I (5′-TCGA overhang, lane 6), and *Xba*I (5′-CTAG overhang, lane 9) fragments varied in the degree to which migration was retarded. The fragments cited above are listed in order from highly retarded to slightly retarded by the electrophoretic conditions. Interestingly, even under the conditions of 1 mM Mg^{2+}, at 37 °C, band shift was observed for *Ban*I, *Mlu*I, *Hga*I, and *Tsp*RI fragments (lanes 7, 10, 19, and 21, respectively). The nine-nucleotide overhang of the *Tsp*RI fragment caused it to be retained in

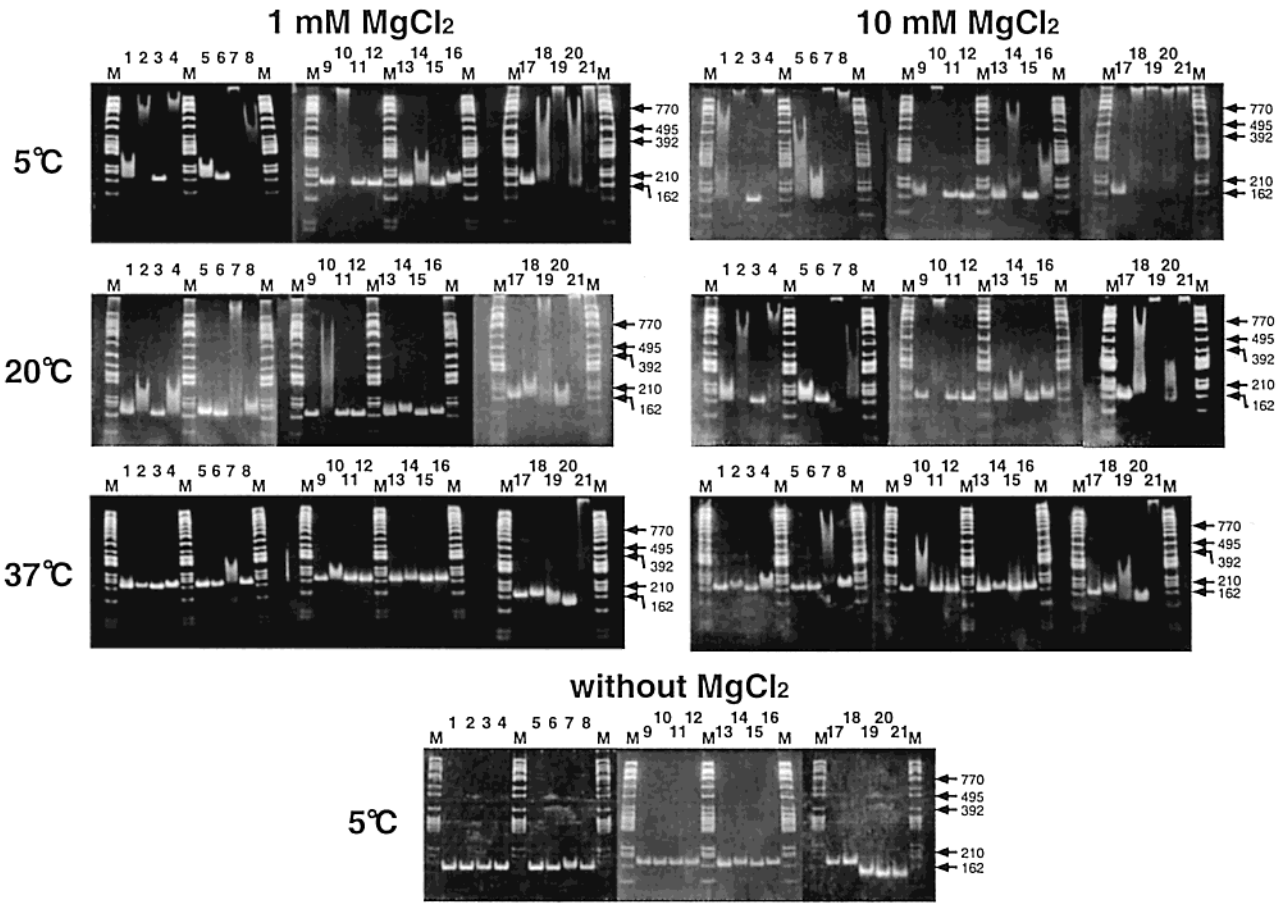

FIGURE 3: Effect of Mg^{2+} on the electrophoretic behavior of various restriction fragments with cohesive ends. Electrophoresis was carried out using 7.5% nondenaturing polyacrylamide gels at 5, 20, or 37 °C in the absence or presence of 1 or 10 mM $MgCl_2$ as indicated in the figure. Lanes are marked according to the fragment numbers in Table 1. Lanes marked M contained marker DNA fragments.

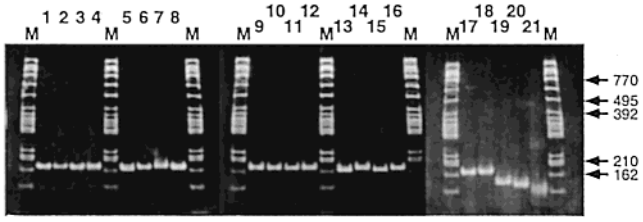

FIGURE 4: Alteration of cohesive ends to blunt results in normal electrophoretic behavior. To generate blunt ends, DNA fragments 1−20 were treated with T4 DNA polymerase and fragment 21 was treated with S1 nuclease. Electrophoresis was carried out using 7.5% nondenaturing polyacrylamide gels at 5 °C in the presence of 10 mM $MgCl_2$. Lanes are marked according to the fragment numbers. Lanes marked M contained marker DNA fragments.

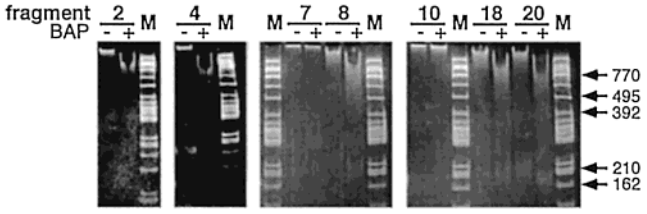

FIGURE 5: Effect of the removal of 5′-phosphate from DNA on mobility. The DNA fragments 2, 4, 7, 8, 10, 18, and 20 were treated with bacterial alkaline phosphatase and subjected to electrophoresis. Electrophoretic conditions were the same as those described in the legend of Figure 4.

the wells of the gel at all Mg^{2+} concentrations that were tested (lane 21 in each panel). All fragments migrated normally when the electrophoresis was carried out using $^1/_2\times$ TB (without Mg^{2+}) at 5 °C as shown at the bottom of Figure 3.

We also tested the effect of $CaCl_2$ and NaCl on the electrophoretic mobility of several fragments listed in Table 1. The effect of $CaCl_2$ was almost comparable to that of $MgCl_2$. In the case of NaCl, however, even 100 mM NaCl did not affect the electrophoretic mobility of the restriction fragments (not shown).

Cohesive Ends Are Responsible for the Retarded Migration. The cohesive ends of each fragment were made blunt using T4 DNA polymerase or S1 nuclease, and the resulting fragments were subjected to electrophoresis. All fragments migrated normally in the buffer containing 10 mM Mg^{2+} at 5 °C (Figure 4), which demonstrated that the cohesive ends were responsible for the retarded migration. Subsequently, the effect of the terminal phosphate upon fragment migration was also investigated using the DNA fragments that showed highly retarded migration in Figure 3. As shown in Figure 5, dephosphorylation reduced the level to which migration was retarded for all fragments, although the effect was very slight for the *Ban*I and *Mlu*I fragments (fragments 7 and 10, respectively). This result indicated that the phosphate at the terminus of the overhang was also implicated in the band shift phenomenon.

Base Pairing between Overhangs Is the Cause of the Phenomenon. The efficiency of the ligation reaction was assessed using T4 DNA ligase, and the results are shown in

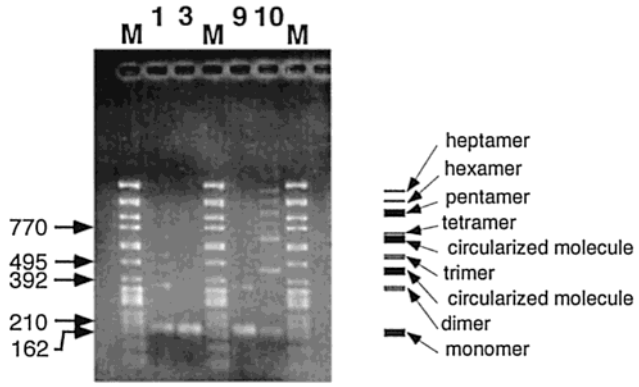

FIGURE 6: Ligation efficiency of a DNA fragment is proportional to the extent of its retarded migration. DNA fragments with different electrophoretic anomalies were subjected to the ligation reaction, which was carried out at 5 °C in the buffer containing 10 mM Mg^{2+}. The products were separated on a 1.5% agarose gel run in $^1/_2\times$ TBE. Lanes are marked according to the fragment numbers. The emergent bands in the lane corresponding to fragment 10 are drawn schematically on the right-hand side.

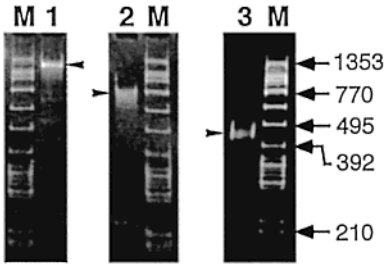

FIGURE 7: DNA fragments with one blunt end and the other 5′-CGCG overhang form dimer in the presence of 10 mM $MgCl_2$. The pPRT-5/4B-derived 583 and 411 bp fragments and the pPRT-5/4U-derived 231 bp fragment were loaded onto lanes 1−3, respectively. Electrophoretic conditions were the same as those described in the legend of Figure 4.

Figure 6. After the reaction, the *Mlu*I fragment (fragment 10) formed oligomers and putative circularized molecules as indicated in the figure. The efficiency of the reaction was found to decrease, in order, from the *Mlu*I fragment (lane 10), to the *Eco*RI fragment (lane 1), to the *Xba*I fragment (lane 9), to the *Afl*II fragment (lane 3), which was the order in the extent of retarded migration in Figure 3. Thus, this result indicates that DNA fragments with certain overhangs are easily oligomerized in the presence of Mg^{2+} through stable base pairing. This interpretation was further strengthened by the results shown in Figures 7 and 8. Figure 7 shows dimerization of the fragments using a DNA fragment with one blunt end and the other having a 5′-CGCG overhang. All bands shifted to the position corresponding to the dimer of each fragment. The fragment shown in lane 2 migrated slightly faster than the migration expected for the dimer. This appears to have been caused by the fast-migrating property of the "monomer" fragment subjected to the electrophoresis, which is 411 bp but behaved as 400 bp molecules when electrophoresis was performed in the absence of Mg^{2+} (not shown). The existence of such fast-migrating fragments is well-known (*14*−*17*). Direct evidence that oligomer formation is the cause of the band shift is shown in Figure 8. The retarded migration depended on the concentration of DNA molecules in the sample DNA solution that was subjected to electrophoresis. Fragment 10 was found to migrate normally when the DNA concentration was diluted to 0.1 ng/μL. However, when unlabeled DNA was added to the solution in a stepwise fashion, an increased level of retardation of the DNA band was observed, and this was dependent on the concentration of the unlabeled DNA. This result clearly shows that the retarded migration was caused by intermolecular interactions.

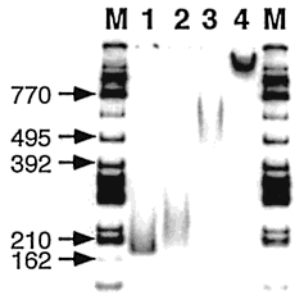

FIGURE 8: Retarded migration disappears after dilution of the sample DNA solution subjected to electrophoresis. Fragment 10, which carries the 5′-CGCG overhangs, was end labeled with [γ-^{32}P]-ATP. In lane 1, 3 μL of a solution containing 0.3 ng of the labeled fragment, $^1/_2\times$ TB, and 1 mM $MgCl_2$ was loaded into the well. In addition to the components in the sample of lane 1, 3 (lane 2), 30 (lane 3), or 300 ng (lane 4) of nonlabeled fragment 10 was included in the solution. Electrophoresis was carried out on 7.5% nondenaturing polyacrylamide gels at 5 °C in the presence of 1 mM $MgCl_2$.

The Stability of the Base Pairing between Overhangs Can Be Roughly Estimated but Not Exactly. The 5′-overhangs 5′-TTAA, 5′-TTA (or 5′-TAA), 5′-TGA (or 5′-TCA), 5′-CG, 5′-TA, and 5′-G (or 5′-C) did not cause band shift under any of the electrophoretic conditions that were tested. Excluding these from the analysis, we estimated the relative stabilities in base pairing from the data shown in Figure 3. According to the thermodynamic parameters reported by Sugimoto et al. (*18*), which were established on the basis of the measurement of the melting curves of double-stranded DNA molecules in the presence of 1 M Na^+, we calculated the stability of the base pairing between complementary overhangs. The expected order of the stability is shown in the lower row in Figure 9. In the upper row, the order is shown as judged from the degree to which the retarded migration occurred. The corresponding overhangs are connected by lines. As shown in the figure, 5′-GCGC and 5′-AATT were more stable than expected and 5′-TCGA and 5′-CTAG were less stable than expected. The stability of the duplex formed by cohesive ends may have been significantly influenced by the stacking interactions of the terminal base of the overhang with the adjacent base in the other partner of the joined ends. As a step in exploring the implication of this putative effect, the predicted stability for the 6 bp steps was also calculated. However, this calculation did not improve the mismatches between predicted and actual stabilities (not shown).

DISCUSSION

The study reported here has shed light on the interaction between the cohesive ends of DNA restriction fragments in the presence of Mg^{2+}. It was concluded that the Mg^{2+}-mediated stable adhesion between short overhangs caused mobility shift of the restriction fragments. Although the electrophoretic detection of the association between tetranucleotide and tRNA was reported in the 1970s (*19*), this is the first report describing electrophoretic detection of

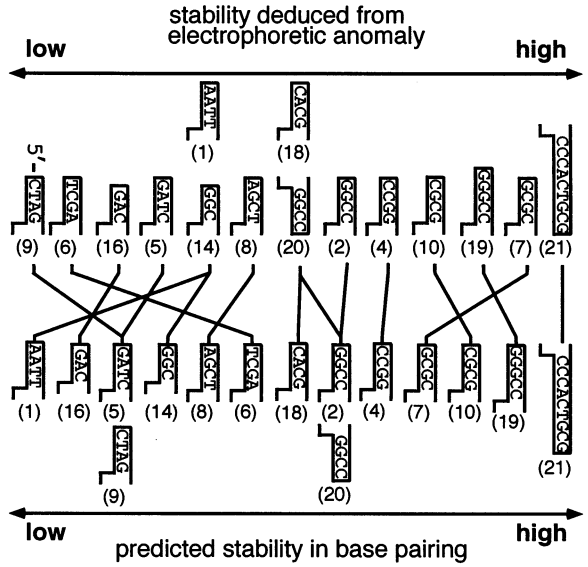

FIGURE 9: Extent of the stability in base pairing between overhangs. The observed order of stability (Figure 3) is shown in the upper row, and the expected order, according to Sugimoto et al. (*18*), is shown in the lower row. The same overhangs are connected by lines. Numerals are the fragment numbers.

intermolecular association between short overhangs of large DNA fragments. The following report is consistent with our conclusion. Using atomic force microscopy (AFM) and electron microscopy, Révet and Fourcade (*20*) demonstrated that restriction fragments carrying overhangs were apt to be circularized by addition of Mg^{2+} or Ca^{2+} at room temperature. In the case of the 3005 bp *Ngo*MI-cleaved plasmid DNA (overhangs, 5′-CCGG), 95% of the DNA fragments maintained a circular conformation in the presence of Mg^{2+}. They also presented electrophoretic data obtained by agarose gel electrophoresis in TAE buffer containing Mg^{2+}. When four differently cleaved plasmid DNA samples were compared, the above *Ngo*MI-cleaved plasmid showed a marked "trace" of the intramolecular end-to-end interaction, which emerged as a smear band between the positions of the linear and nicked molecules.

Our study demonstrated that some of the oligomerized molecules (or their circularized forms) were stable enough under the polyacrylamide gel electrophoresis conditions; i.e., they were resistant to the friction with the gel matrix and were not separated. The relative stabilities in the base pairings between the overhangs generally agreed well with the expected values (Figure 9). This means that by using Mg^{2+}, we could only "magnify" the normal phenomenon of base pairing on the "stage" that we could observe. This also suggests that the stabilities in the base pairing between 3′-overhangs are the same as those between their corresponding 5′-overhangs. The discrepancy observed for the 5′-GCGC, 5′-AATT, 5′-TCGA, and 5′-CTAG overhangs in Figure 9 may be caused by some unknown stabilization or destabilization effect lying between the base at the 5′-end of the overhang of one molecule and the last base of the double-stranded region of the "partner" molecule. Several fragments showed a slight retardation in 10 mM $MgCl_2$ at 5 °C (for example, fragments 6, 9, and 16 in Figure 3). This can be explained by assuming that the considerable amounts of oligomerized fragments or the circularized form of the oligomer dissociated to the "monomer" during the early stage of migration. Fragments 1, 5, and 14 showed an intermediate level of retarded migration (Figure 3). In these cases, it seems that the oligomerized fragments were more resistant to dissociation but were partially (or completely) dissociated in time. The smear patterns observed for both cases appear to reflect this putative molecular event well.

Magnesium ions normally serve a structural role by stabilizing the sugar−phosphate backbone of DNA (*8*). The favored sites for direct coordination to magnesium are phosphate oxygen and N7 and O6 of guanosine (*21*, *22*). Mechanistically, the divalent magnesium alleviates electrostatic repulsive interactions between phosphates, thereby stabilizing base pairing and base stacking (*8*). In this study, the 5′-dephosphorylated overhangs produced a slightly less stable base pairing than their phosphorylated counterparts (Figure 5). Although we cannot explain the precise mechanism by which this phenomenon occurs, magnesium ion stabilization of the sugar−phosphate backbone seems to be related. In relation to the effect of 5′-terminal phosphate, the following report has been presented. The 5′-dephosphorylated overhangs 5′-GGCC, 5′-GCGC, and 3′-GCGC appear to retard migration of the fragments in the nondenaturing polyacrylamide gels, even without Mg^{2+}, in an end-to-end interaction-independent manner (*23*). The extent of this retardation, however, was much smaller than that derived from oligomerization as observed in this study.

We must be careful in the interpretation of the mobility data when we perform electrophoresis in the presence of magnesium or calcium ions. We have reported data related to this caution, which were obtained by electrophoretic analysis at 5 °C in the presence of 10 mM $MgCl_2$ or $CaCl_2$ (*14*). At that time, we had already noticed the migration phenomenon reported here. Therefore, we made all permuted fragments blunt ended to prevent misinterpretation (conversion of cohesive ends to blunt ends is the easiest way to deal with this problem). Many papers have been published without knowledge of the phenomenon described here. On the basis of the mobility data of several synthetic DNA fragments with the four-nucleotide overhangs in the presence of 10 mM $MgCl_2$, Bruckner et al. (*10*) reported that a physiological concentration of magnesium ions induces a strong macroscopic curvature in GGGCCC-containing DNA. However, in light of this study, some misinterpretation of the data may be involved. The report by Dlakic and Harrington (*12*) contrasts with the above report. They studied the effects of sequence context on the formation of DNA curvature. In their study, they performed a similar electrophoresis. However, since the overhangs of their DNAs were 5′-AGA and 5′-TCT in which the effect on base pairing is presumably very weak, it is supposed that the band shift did not originate from the interaction between the overhangs. In a study by Diekmann (*24*), the magnesium dependence of the gel migration anomaly of intrinsically bent DNA fragments was investigated, where restriction fragments generated by *Hae*III (blunt) or *Eco*RI (5′-AATT) were used. The results for the *Eco*RI fragments may partly exhibit the effect of the end-to-end interaction. Furthermore, a *Hin*dIII fragment of kinetoplast DNA (bent DNA) was reported to show unusually large *k*-factors (apparent size divided by actual size) in the presence of 5−20 mM $MgCl_2$ without apparent explanation (*25*). This can be explained in terms

of the highly stabilized base pairing between the overhangs as clarified in this study.

Several overhangs did not cause the retarded migration of the restriction fragments (Figure 3). This may not be because they could not stabilize the intermolecular (or intramolecular) end-to-end interactions, but because their interaction was very weak and thus the dissociation of the interacting fragments occurred more easily during electrophoresis. The Mg^{2+}-mediated stabilization of base pairing between overhangs appears to allude to the presence of a fundamental mechanism in living cells that supports many basic genetic processes to be performed accurately and that protects genomes from mutation caused by accidental cleavage.

ACKNOWLEDGMENT

We thank H. Tsujibayashi for technical assistance and J. Ohyama for help in preparing the manuscript.

REFERENCES

1. Sambrook, J., Fritsch, E. F., and Maniatis, T. (1989) *Molecular Cloning: A Laboratory Manual*, 2nd ed., Cold Spring Harbor Laboratory Press, Plainview, NY.
2. Carey, M., and Smale, S. T. (2000) *Transcription Regulation in Eukaryotes: Concept, Strategies, and Techniques*, Cold Spring Harbor Laboratory Press, Plainview, NY.
3. Marini, J. C., Levene, S. D., Crothers, D. M., and Englund, P. T. (1982) *Proc. Natl. Acad. Sci. U.S.A. 79*, 7664−7668.
4. Diekmann, S., and Lilley, D. M. J. (1987) *Nucleic Acids Res. 15*, 5765−5774.
5. Wu, H. M., and Crothers, D. M. (1984) *Nature 308*, 509−513.
6. Ohyama, T. (2001) *BioEssays 23*, 708−715.
7. van der Vliet, P. C., and Verrijzer, C. P. (1993) *BioEssays 15*, 25−32.
8. Cowan, J. A. (1995) *The Biological Chemistry of Magnesium*, VCH Publishers, New York.
9. Nickol, J., and Rau, D. C. (1992) *J. Mol. Biol. 228*, 1115−1123.
10. Brukner, I., Susic, S., Dlakic, M., Savic, A., and Pongor, S. (1994) *J. Mol. Biol. 236*, 26−32.
11. Shimizu, M., Kubo, K., Matsumoto, U., and Shindo, H. (1994) *J. Mol. Biol. 235*, 185−197.
12. Dlakic, M., and Harrington, R. E. (1996) *Proc. Natl. Acad. Sci. U.S.A. 93*, 3847−3852.
13. Han, W., Lindsay, S. M., Dlakic, M., and Harrington, R. E. (1997) *Nature 386*, 563.
14. Ohyama, T., Tsujibayashi, H., Tagashira, H., Inano, K., Ueda, T., Hirota, Y., and Hashimoto, K. (1998) *Nucleic Acids Res. 26*, 4811−4817.
15. Anderson, J. N. (1986) *Nucleic Acids Res. 14*, 8513−8533.
16. Milot, E., Belmaaza, A., Wallenburg, J. C., Gusew, N., Bradley, W. E. C., and Chartrand, P. (1992) *EMBO J. 11*, 5063−5070.
17. Fitzgerald, D. J., Dryden, G. L., Bronson, E. C., Williams, J. S., and Anderson, J. N. (1994) *J. Biol. Chem. 269*, 21303−21314.
18. Sugimoto, N., Nakano, S., Yoneyama, M., and Honda, K. (1996) *Nucleic Acids Res. 24*, 4501−4505.
19. Eisinger, J., and Blumberg, W. E. (1973) *Biochemistry 12*, 3648−3662.
20. Révet, B., and Fourcade, A. (1998) *Nucleic Acids Res. 26*, 2092−2097.
21. Ho, P. S., Frederick, C. A., Quigley, G. J., van der Marel, G. A., van Boom, J. H., Wang, A. H., and Rich, A. (1985) *EMBO J. 4*, 3617−3623.
22. Gessner, R. V., Quigley, G. J., Wang, A. H., van der Marel, G. A., van Boom, J. H., and Rich, A. (1985) *Biochemistry 24*, 237−240.
23. Muiznieks, I., and Doerfler, W. (1998) *Nucleic Acids Res. 26*, 1899−1905.
24. Diekmann, S. (1987) *Nucleic Acids Res. 15*, 247−265.
25. Diekmann, S., and Wang, J. C. (1985) *J. Mol. Biol. 186*, 1−11.

BI026308F